

Evolution of the Precipitation Kinetics, Morphology, and Permeation Performance of Phenolphthalein Poly(ether sulfone) Hollow-Fiber Membranes with Polyvinylpyrrolidones of Different Molecular Weights as Additives

Wan-Zhong Lang, Lian-Feng Chu, Ya-Jun Guo

Department of Chemistry, Shanghai Normal University, 100 Guilin Road, Shanghai 200234, China

Received 18 August 2009; accepted 14 November 2010

DOI 10.1002/app.33753

Published online 14 March 2011 in Wiley Online Library (wileyonlinelibrary.com).

ABSTRACT: Phenolphthalein poly(ether sulfone) (PES-C) hollow-fiber ultrafiltration (UF) membranes were fabricated by wet spinning and dry-jet/wet spinning (10-cm air gap) processes with polyvinylpyrrolidones (PVPs) of different molecular weights as additives. Light transmittance experiments were performed to obtain insight into the precipitation kinetics of PES-C/PVP/*N*-methyl-2-pyrrolidone (NMP) dope solutions. The morphology and permeation performance of the prepared PES-C hollow-fiber membranes were well characterized and elucidated with scanning electron microscopy and UF experiments in addition to the precipitation kinetics. The thermal and mechanical properties of the membranes were also studied. Experiments demonstrated that all PES-C/PVP/NMP dope solutions experienced instantaneous demixing with pure water as the coagulant, and the precipitation rate decreased as the molecular weight of PVP increased. A double, finger-like structure occurred in the PES-C hollow-fiber membranes spun with PVPs of low molecular weight (10,000, 24,000, or 58,000) as additives; however, a spongelike

structure occurred in the PES-C membranes with PVP with a molecular weight of 1,300,000 because of its very low precipitation rate. The pure water permeation (PWP) flux decreased and the rejection of lysozyme increased for the prepared PES-C membranes as the molecular weight of PVP increased. The largest PWP flux of $149 \text{ L m}^{-2} \text{ h}^{-1} \text{ bar}^{-1}$ was acquired for dry-jet/wet-spun PES-C membranes with PVP with a molecular weight of 10,000 as an additive. The rejection of bovine serum albumin for the prepared PES-C membranes was greater than 98%, and the rejection of lysozyme ranged from 47.1 to 89.4%; this indicated typical UF membranes. The decomposition temperature of the PES-C membranes containing PVP was lower than that of the original polymer and decreased as the molecular weight of PVP increased. The break strain and the elongation at break were enhanced as the PVP molecular weight increased. © 2011 Wiley Periodicals, Inc. *J Appl Polym Sci* 121: 1961–1971, 2011

Key words: fibers; membranes; separation techniques

INTRODUCTION

Ultrafiltration (UF) is an attractive separation process because it is simple, energy-saving, and easy to operate. With the exigent demands of energy savings and emission reductions, UF membrane technology has been highly valued in recent years. Many polymers, including polysulfone (PSf), poly(ether sulfone) (PES), polyacrylonitrile (PAN), and poly(vinylidene fluoride), have been involved in

the fabrication of UF membranes by non-solvent-induced phase separation.^{1,2}

Phenolphthalein poly(ether sulfone) (PES-C) is a relatively newly developed engineering thermoplastic.³ Its chemical structure is shown in Figure 1. As can be seen from its chemical structure, PES-C can be considered a PES modified by the introduction of rather bulky and polarizable phenolphthalein groups in place of oxygen atoms. In comparison with PES and PSf polymers, PES-C has better hydrophilicity, thermal stability, and mechanical properties for the introduction of phenolphthalein groups. Because of its excellent performances, it has been sulfonated and used as a membrane material for gas permeation,⁴ UF/nanofiltration,⁵ and fuel cells⁶ and has been blended with other polymers for membrane preparation.^{7,8}

For a specific membrane material, an effective method for adjusting the membrane structure and fine-tuning its performance involves the introduction of an additive into a dope solution and the

Correspondence to: W.-Z. Lang (wzlang@shnu.edu.cn).

Contract grant sponsor: Leading Academic Discipline Project of Shanghai Normal University; contract grant number: DZL807.

Contract grant sponsor: Shanghai Municipal Natural Science Foundation; contract grant number: 09ZR1423300.

Contract grant sponsor: National Natural Science Foundation of China; contract grant number: 20906062.

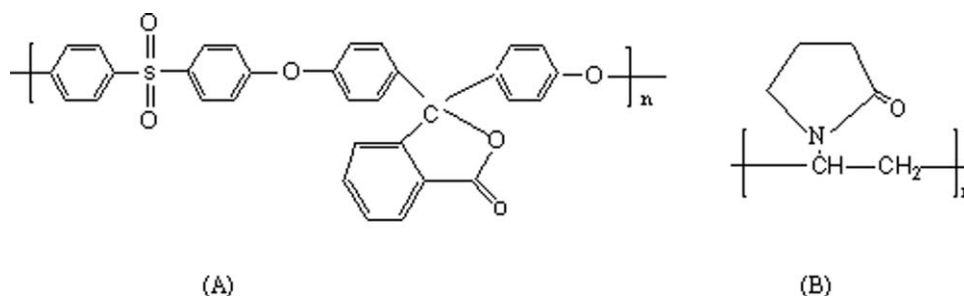


Figure 1 Chemical structures of (A) PES-C and (B) PVP.

regularization of the phase-separation process via the tuning of the thermodynamics and precipitation kinetics of the dope solution.^{9–17} Many researchers have investigated the addition of an organic or inorganic, small- or large-molecule constituent as the third component in a polymeric dope/cast solution. Xu and Qusay¹³ investigated a small alcohol as a nonsolvent additive for the preparation of a single-skin PES hollow-fiber membrane. The experimental results illustrated that the PES membrane morphology changed slowly from a long and wide, fingerlike structure to a spongelike structure with some macrovoids as the ethanol concentration in the dope solution increased. Li et al.¹⁴ and Chakrabarty et al.¹⁵ prepared flat PES and PSf membranes, respectively, with poly(ethylene glycol)s (PEGs) of different molecular weights as additives. Li et al.'s experimental results revealed that PES membranes prepared with PEG400 (i.e., PEG with a molecular weight of 400 Da) and PEG600 as additives had no microspores on the top surface, but the membranes prepared with PEG200 as an additive had microspores. Chakrabarty et al.'s results showed that the pore number and the pore area of the membranes increased with increasing PEG molecular weight. The membranes prepared with high-molecular-weight PEG as an additive had high pure water permeation (PWP) flux and hydraulic permeability. Idris et al.¹⁶ also prepared flat PES UF membranes with PEGs of different molecular weights as additives, and results similar to Li et al.'s observations were obtained. Susanto and Ulbricht¹⁷ prepared flat PES UF membranes with polyvinylpyrrolidone (PVP), PEG, and poly(ethylene oxide)-*b*-poly(propylene oxide)-*b*-poly(ethylene oxide) as macromolecular additives, and the effects of the different additives on the membrane structure and permeation performance were investigated.

PVP is an important pore-forming agent in membrane formation.^{9,10,18–20} The molecular weight and content of PVP in the dope solution have a great influence on the morphology and permeation performance of the resultant membrane. Yang and coworkers^{18–20} investigated the preparation of PES hollow-fiber membranes for hemofiltration with

PVPs of different molecular weights as additives and found that macrovoids in the PES membrane cross section could not be eliminated when the membranes were spun without PVP or with a low-viscosity dope containing PVP of a low molecular weight. The PES hollow-fiber membrane changed from a three-layer structure to a double, fingerlike structure to a spongelike structure when the concentration of PVP (molecular weight = 360,000) was increased from 0 to 5 to 10% in the dope solution. Ochoa et al.²¹ found that the addition of small quantities of PVPs of different molecular weights to PES casting solutions resulted in an increase in the permeability without a significant change in the selectivity. Jung et al.²² prepared flat PAN membranes with PVPs of different molecular weights as additives; they found that the top layers were thicker when more PVP was added, and the macrovoids gradually disappeared. Also, the thickness of the top layer increased when a PVP of a higher molecular weight was added.

Even though PES-C has excellent mechanical and thermal properties, to the best of our knowledge, work about membranes directly prepared from PES-C has been rarely reported, and even less has been reported about hollow-fiber UF membranes. It is well known that the hollow-fiber membrane configuration is the most favored membrane module. In comparison with flat and tubular membranes, hollow-fiber membranes have a larger membrane area per unit of volume of the membrane module, and they offer higher productivity per unit of volume. However, the preparation of hollow-fiber membranes involves more factors than flat-sheet membranes during membrane fabrication, such as internal/external coagulation solutions and a large number of spinning parameters (e.g., the structure and dimensions of the spinneret, the polymer dope viscosity, the flow rate of the bore fluid, the dope extrusion rate, the length of the air gap, and the take-up speed). Therefore, an attempt was made to fabricate PES-C hollow-fiber UF membranes with four PVPs of different molecular weights as additives. The aforementioned descriptions indicate that PVP is a fine additive and hydrophilizing and pore-

TABLE I
Spinning Conditions for the PES-C Hollow-Fiber Membranes

No.	Membrane	Dope solution composition	Viscosity (Pa s)	Inner/external coagulation fluid	Air gap (cm)
1	K15-WW	18/5/77 PES-C/PVP (K15)/NMP	19.5	H ₂ O/H ₂ O	0
2	K15-DW				10
3	K25-WW	18/5/77 PES-C/PVP (K25)/NMP	23.6	H ₂ O/H ₂ O	0
4	K25-DW				10
5	K30-WW	18/5/77 PES-C/PVP (K30)/NMP	25.6	H ₂ O/H ₂ O	0
6	K30-DW				10
7	K90-WW	18/5/77 PES-C/PVP (K90)/NMP	>100	H ₂ O/H ₂ O	0
8	K90-DW				10

forming agent for polymeric membranes. It has been verified that PVP and PES-C are miscible over the entire composition range.²³ This provides the basis for fabricating PES-C membranes with PVP as an additive in this research.

In this case, wet spinning (wet/wet) and dry-jet/wet spinning (dry/wet; 10-cm air gap) were used in the preparation of PES-C hollow-fiber membranes. The evolution of the precipitation kinetics, morphology, and permeation performance of PES-C hollow-fiber membranes with PVPs of different molecular weights as additives were investigated in detail. The thermal and mechanical properties were also studied.

EXPERIMENTAL

Materials

PES-C (specific viscosity/concentration = 0.9, glass-transition temperature = 260°C) in a powder form was purchased from Xuzhou Engineering Plastic Co., Ltd. (Xuzhou, People's Republic of China). PVP K15 [weight-average molecular weight (M_w) = 10,000], PVP K25 (M_w = 24,000), PVP K30 (M_w = 58,000), and PVP K90 (M_w = 1,300,000) were purchased from Shanghai Jinchun Chemical Agent Co., Ltd. (Shanghai, People's Republic of China). Bovine serum albumin (BSA; M_w = 67,000) and lysozyme (M_w = 14,400) from Shanghai Bio Life Science and Technology Co., Ltd. (Shanghai, People's Republic of China), and the solvent *N*-methyl-2-pyrrolidone (NMP) from Shanghai Chemical Agent Co. Ltd. (Shanghai, People's Republic of China) were obtained.

Preparations of the dope solutions and hollow-fiber membranes

PES-C and PVP were first dried at 70°C for more than 48 h. Then, the acquired amounts of dried PES-C and PVPs of different molecular weights were added to the solvent in a glass bottle. The PES-C/PVP/NMP mixtures were stirred at 70°C until homogeneous solutions were obtained.

PES-C hollow-fiber membranes were fabricated by wet/wet and dry/wet processes at room temperature. The prepared spinning dope solution was first kept in a tank overnight for degassing before spinning. The dope solution and bore fluid passed through a spinneret (orifice diameter = 0.9 mm, inner diameter of the tube = 0.5 mm) at the pressure of N₂ and through a constant-flow pump, respectively. The ratio of the dope flow rate to the bore fluid flow rate was constant in all spinning processes. The nascent fibers were not drawn (no extension); that is, the take-up velocity of the hollow-fiber membranes was nearly the same as the falling velocity in the coagulation bath. The PES-C membranes were stored in a water bath for 24 h to remove residual NMP. After this period, the fibers were posttreated in an aqueous solution of 50 wt % glycerol for 24 h to prevent the collapse of porous structures and were dried in air at room temperature during the making of the test modules. The dope solution compositions, bore fluids, and spinning conditions for the preparation of the PES-C hollow-fiber membranes are summarized in Table I. The prepared membranes were coded by the type of PVP, with WW and DW representing fibers spun by the wet/wet and dry/wet processes, respectively.

Light transmittance measurements

The precipitation kinetics of PES-C solutions with PVPs of different weights as additives was studied with light transmittance experiments. A schematic diagram of this equipment is shown in Figure 2. The PES-C dope was first cast onto glass and then immediately immersed into a water bath, which acted as a coagulation fluid. The water bath temperature was room temperature (20°C). The light source of a laser was directly exposed to a cast dope approximately 20 cm above it. The transmitted light was detected with an optical detector. The accepted signal was then analog to digital (A/D)-converted, amplified, and recorded by a computer. The intensity of the transmitted light through the cast dope was measured as a function of time.

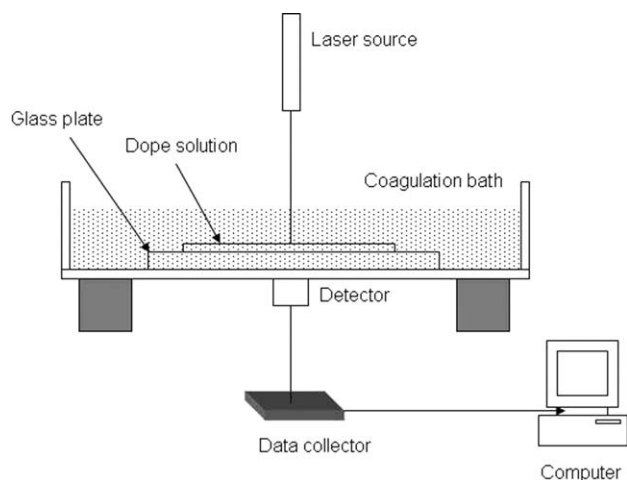


Figure 2 Schematic diagram of the setup for coagulation kinetics.

Membrane characterization

Membrane morphology of the PES-C UF hollow-fiber membranes

The morphology of the hollow-fiber membranes was examined with scanning electron microscopy (SEM; JSM-6380 LV, JEOL, Tokyo, Japan). The fibers were first immersed into liquid nitrogen for a few minutes and were then broken and deposited onto a copper holder. All samples were coated with gold *in vacuo* before the testing.

Permeation and separation performances of the PES-C hollow-fiber UF membranes

The permeation and separation performances of the prepared PES-C membranes were measured with UF experiments. BSA and lysozyme solutions (500 ppm), respectively, were chosen as the feed fluids.

All experiments were conducted at room temperature with a feed pressure of 1.0 bar with a self-made UF experiment setup, which is shown in Figure 3. The concentrations of the permeate and feed of BSA and lysozyme were determined at 280 nm with a UV spectrophotometer (UV-3000, Shimadzu, Kyoto, Japan). The PWP flux and rejection of the membranes for different solutes are defined as follows:

$$\text{PWP} = \frac{Q}{\Delta P \cdot A} \quad (1)$$

$$R = \left(1 - \frac{C_P}{C_F}\right) \times 100\% \quad (2)$$

where PWP is the permeation flux of the membrane for pure water ($\text{L m}^{-2} \text{h}^{-1} \text{bar}^{-1}$); Q is the volumetric flow rate of pure water (L/h); ΔP is the transmembrane pressure (bar); A is the effective area of the membranes (m^2); R is the rejection of the membrane for different solutes; and C_P and C_F are the permeate and feed concentrations, respectively.

Thermal analysis

The thermal properties of the prepared PES-C membranes were evaluated by thermogravimetric analysis (TGA; DSCQ100, TA Co., New Castle United States). The TGA measurements were carried out under a nitrogen atmosphere at a heating rate of $10^\circ\text{C}/\text{min}$ from 25 to 700°C .

Mechanical property test

To investigate the mechanical properties, the break strain and elongation at break of the prepared PES-C hollow-fiber membranes were tested with an AG-1 material test machine (Shimadzu) at a loading

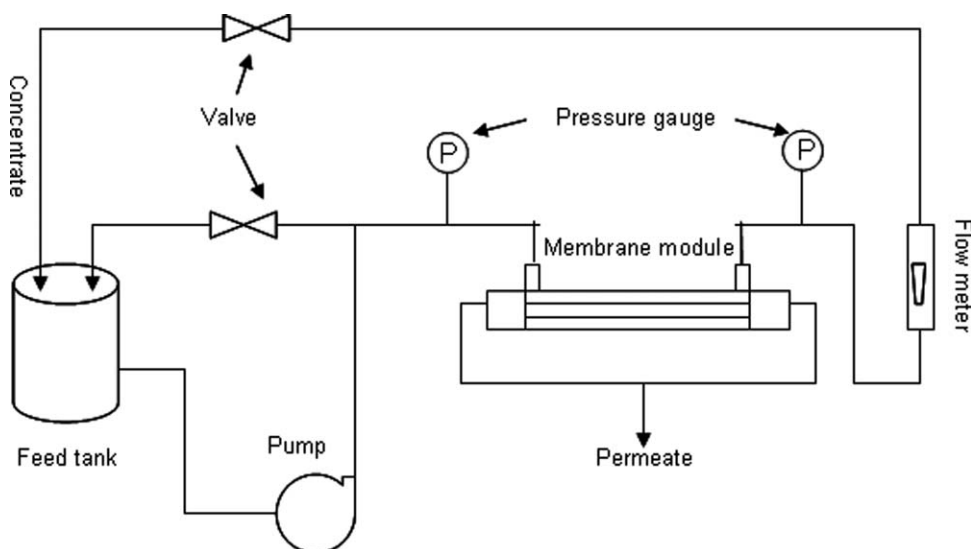


Figure 3 Schematic diagram of the UF experiment.

velocity of 50 mm/min. Each fiber sample was tested 10 times, and the mean values and error were presented.

RESULTS AND DISCUSSION

Precipitation kinetics of the PES-C/PVP/NMP dope solutions

On the basis of different delay times, precipitation processes can be divided into instantaneous demixing and delayed demixing. A process involving instantaneous demixing is characterized by an instantaneous decrease in the light transmission, which indicates the generation of many scattering nuclei.^{1,24,25} Light transmittance experiments were applied to measure the precipitation kinetics of PES-C/PVP/NMP dope solutions. Deionized water was used as the coagulation fluid. The results are displayed in Figure 4.

In Figure 4, general instantaneous demixing can be observed for four PES-C/PVP/NMP dope solutions containing PVPs of different molecular weights. In addition, it can be seen that the precipitation rate of PES-C/PVP/NMP decreased with the PVP molecular weight increasing. The strong affinity between the solvent (NMP) and the nonsolvent (water) was the cause of the instantaneous demixing of the PES-C/PVP/NMP dope solutions. Furthermore, PVP moved toward the external surface and improved the hydrophilicity during non-solvent-induced phase separation. The improved hydrophilic surface sped the diffusion of the nonsolvent (water) into the dope and led to the instantaneous demixing. Some researchers have also found that the coagulation rate of other polymer dope solutions decreases as the molecular weight of PVP increases.^{18–20,25} This can be explained by the thermodynamics and kinetics of the precipitation process. First, as the molecular weight of PVP increases, the nonsolvent tolerance of the dope solution increases.²⁵ That is, a small nonsolvent variation will cause phase separation for a dope containing a low-molecular-weight PVP. Second, the precipitation rate is mainly controlled by the kinetics.¹⁴ Generally, the viscosity of a dope solution increases with the molecular weight of the polymer. The viscosities of four PES-C/PVP/NMP dope solutions were measured in this case and are listed in Table I. The viscosity of the dope solution increased with the molecular weight of PVP. The different viscosities of the four dope solutions caused the distinct differences in the precipitation rates of the four dopes. The increased viscosity of the dope solution resulted in a decrease in the exchange rate between the solvent and the nonsolvent during the precipitation process. According to this description, it can be accepted that a low-

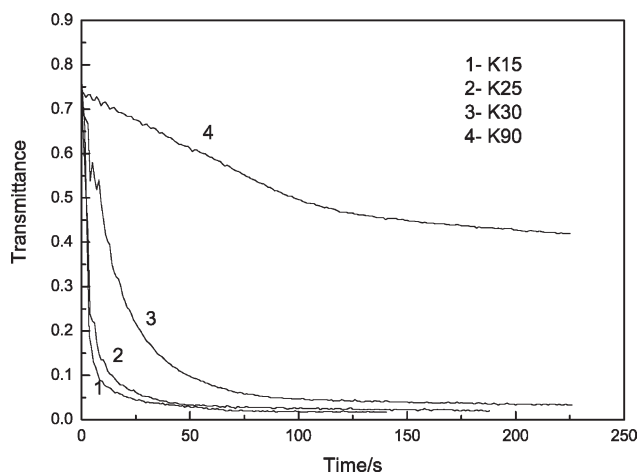


Figure 4 Effects of the molecular weight of PVP on the precipitation kinetics of PSE-C/PVP/NMP dope solutions (with pure water as the coagulation fluid at room temperature).

molecular-weight PVP is favorable for phase separation and precipitation rates both thermodynamically and kinetically. This is the reason that the dope solution containing PVP of a higher molecular weight had a lower precipitation rate. This result accorded with the findings by Kang and Lee²⁵ for PAN dope solutions containing PVPs of different molecular weights.

The exchange rate of the solvent and the nonsolvent between the dope solution and the coagulation fluid plays an important role in determining the morphology and permeation performance of the resultant membranes. Generally, typical instantaneous demixing leads to a fingerlike structure, and delayed demixing leads to a spongelike structure.¹ The relationship between the precipitation kinetics, membrane morphology, and permeation performance for PES-C is discussed later.

Morphologies of the PES-C hollow-fiber membranes

SEM images of the cross-sectional morphologies, external surfaces, and internal surfaces of the prepared PES-C hollow-fiber membranes are displayed in Figures 5–7, respectively.

As shown in Figure 5, double, fingerlike layers were observed for the PES-C hollow-fiber membranes with PVP K15, PVP K25, and PVP K30 as additives for both spinning processes. This was supported by precipitation curves (Fig. 4). Water, acting as a strong nonsolvent, was used for both internal and external coagulation fluids. The fast precipitation rates of the dope solutions led to a fingerlike structure for the resultant membranes. Figure 5 also shows that the fingerlike cavities in the sublayers of the PES-C membranes were

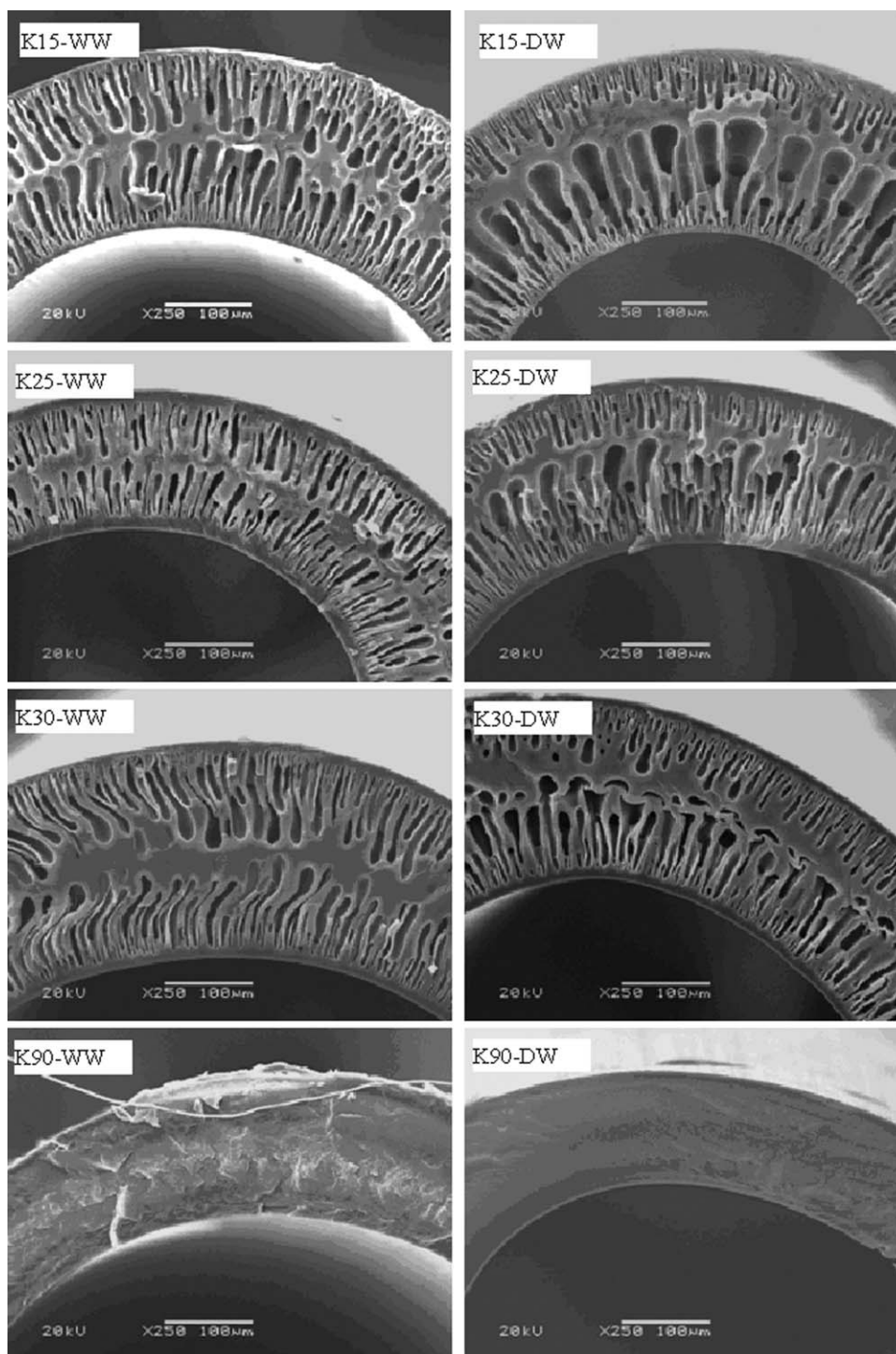


Figure 5 SEM images of the cross-sectional morphologies of the PES-C hollow-fiber membranes.

significantly suppressed with an increase in the molecular weight of PVP in both processes. In particular, the fingerlike cavities and macrovoids disappeared in the PES-C membranes with PVP K90 as an additive.

The morphology of a polymeric membrane made by non-solvent-induced phase separation is affected by many factors: the polymer concentration, the solvent, the additive type and concentration, and the

fabrication conditions (including the air humidity).^{18,26–28} Investigating PES nanofiltration membranes, Boussu et al.^{26,27} found that voids in the cross section were evidently suppressed, and a more spongelike structure formed.^{26,27} Li et al.'s investigation of PES membranes indicated that the cross-sectional morphology changed from a fingerlike structure to a spongelike structure when the precipitation rate decreased.^{14,28} This decrease in the

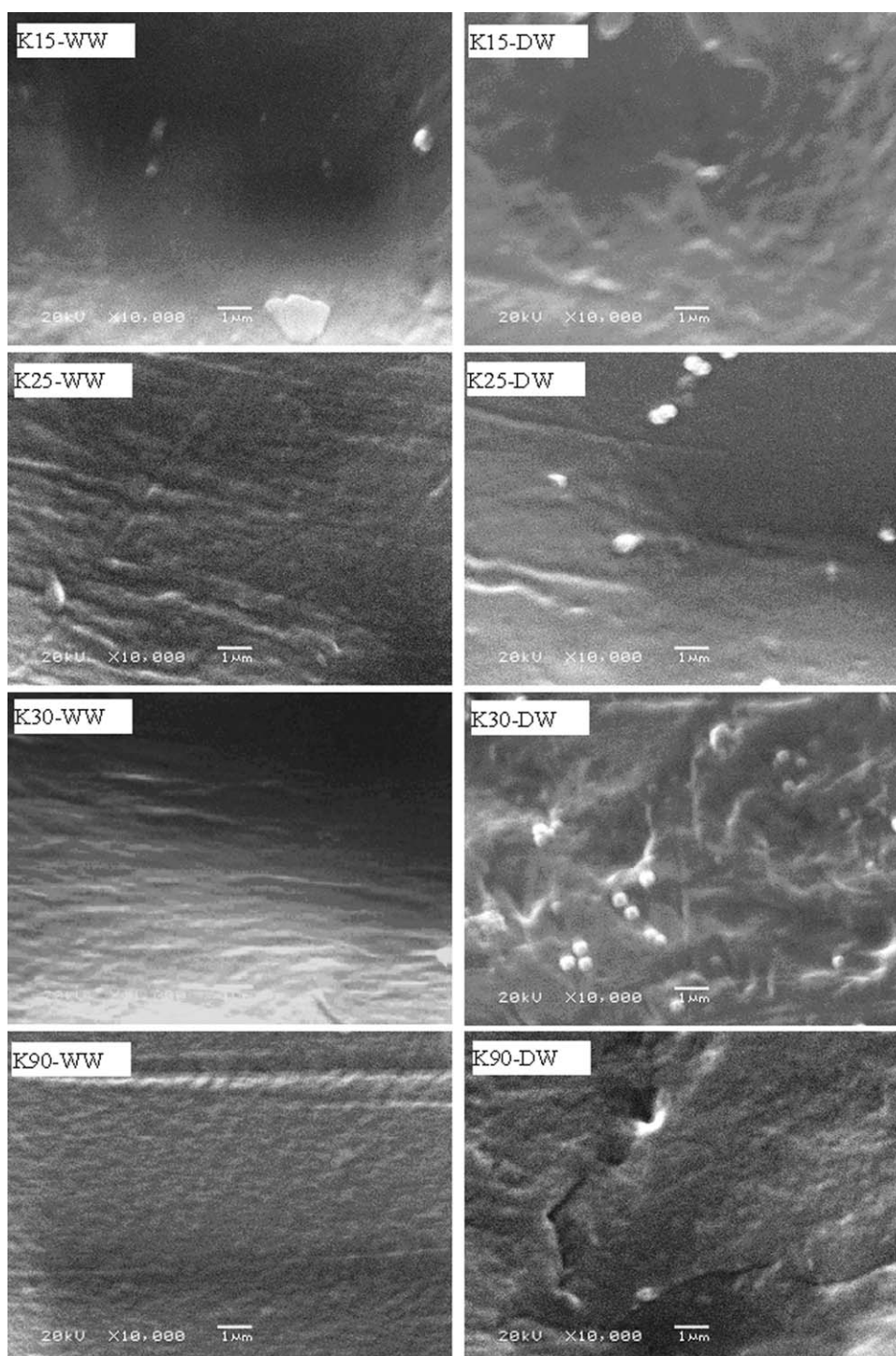


Figure 6 SEM images of the external morphologies of the PES-C hollow-fiber membranes.

precipitation rate was due to the increase in the dope viscosity with the addition of PEG and diethylene glycol to the PES dope solution. Peng et al.²⁹ also claimed the existence of a critical concentration and a corresponding absolute viscosity value in the evolution of macrovoids in the formation of polymeric membranes. Therefore, below the critical point, polymer chains possess a high degree of free-

dom and are loosely packed, and the nonsolvent can easily penetrate the chain spaces of the polymer solution via a diffusional and convective moving front and form macrovoids. As the polymer concentration exceeds the critical value, the polymer chains become closely packed enough to form entanglements. Such an entangled network structure impedes the nonsolvent intrusion and hence lowers

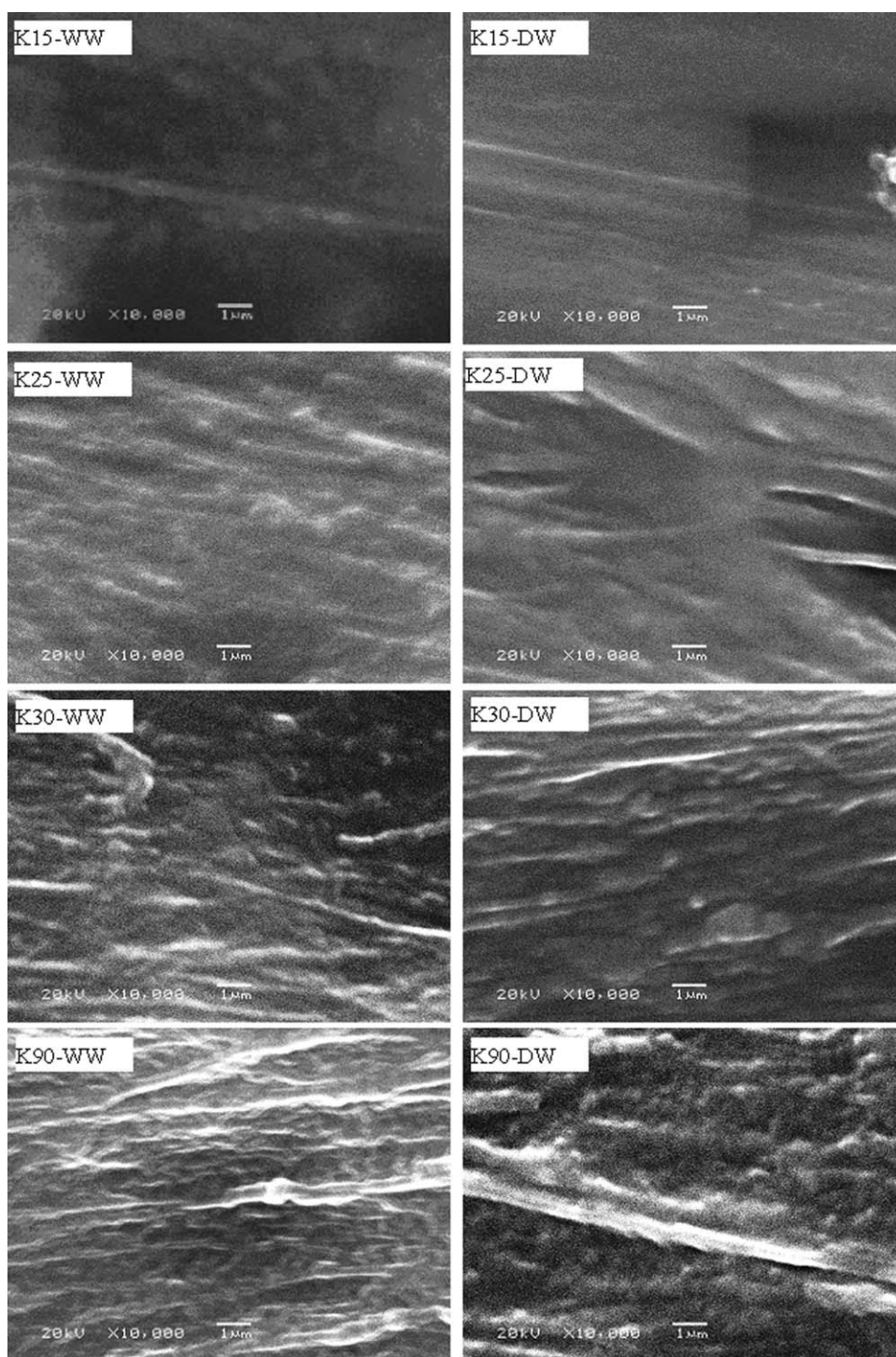


Figure 7 SEM images of the internal surfaces of the PES-C hollow-fiber membranes.

the precipitation rate of the corresponding dope (Fig. 4). In this case, the spongelike structure of the membranes containing PVP K90 should be the result of the ultrahigh viscosity of the dope solution and the very low precipitation rate. According to this discussion, it can be concluded that an increase in the viscosity of the dope solution will lower its precipitation rate during non-solvent-induced phase

separation and will be favorable for the suppression of macrovoids and the formation of a spongelike morphology. Spongelike structures were also found for PES and PSf membranes when a PVP of a very high molecular weight was used as an additive by Yang et al.¹⁸ and Chakrabarty et al.,³⁰ respectively.

The effect of the air gap on the membrane morphology can also be observed in the SEM images of

Figure 5. The lengths of the double, fingerlike cavities of the wet/wet-spun PES-C membranes were almost equal, but the internal fingerlike cavities were significantly longer than the external ones of the dry/wet-spun PES-C membranes. Meanwhile, this difference was enhanced as the molecular weight of PVP decreased. During the wet/wet process, precipitation immediately occurred for both surfaces when the dope solution was extruded from the spinneret. This caused the formation of double, fingerlike cavities of almost equal lengths. However, during the dry/wet process, the onset of precipitation for internal and external surfaces occurred at different times. The precipitation process of the internal surface immediately occurred after the dope solution was extruded from the spinneret, but the external surface went through an air gap and intruded into the external coagulation fluid; then, phase separation occurred. Therefore, the fingerlike cavities of the internal layer were longer than those of the external layer of the PES-C hollow-fiber membranes, as shown in the cross-sectional images of Figure 5. According to optical microscopy observations of the formation of polymer membranes in the literature,^{25,31} the end and length of the fingerlike cavities can be regarded as the precipitation front and precipitation distance, respectively. Because of the increases in the nonsolvent tolerance and viscosity of a polymer solution with an increase in the PVP molecular weight, a dope solution containing PVP of a higher molecular weight has a lower precipitation rate. This was verified by the coagulation kinetics of different dope solutions shown in Figure 4. Therefore, the length of the internal fingerlike cavities was much longer than the length of the external ones for the dope solution containing PVP of a lower molecular weight.

SEM images of the external and internal surfaces of the prepared PES-C hollow-fiber membranes are shown in Figures 6 and 7, respectively. Because water acting as a strong nonsolvent was involved as an internal and external coagulation bath, a dense skin was observed on both surfaces. Another phenomenon was that both the external and internal surfaces became rougher when the molecular weight of PVP increased in the PES-C membranes. This can be explained as follows: the high viscosity of the dope solution caused by the addition of high-molecular-weight PVP restricted the relaxation and orientation of the molecular chains of the polymer.^{21,32,33}

Permeation and separation performances of the PES-C membranes

The PWP flux and rejection for two proteins (BSA and lysozyme) for the prepared PES-C hollow-fiber membranes are listed in Table II. The PWP flux

TABLE II
Permeation Flux and Rejection of Solutes of the PES-C Hollow-Fiber Membranes

Membrane	PWP (L m ⁻² h ⁻¹ bar ⁻¹)	Rejection (%)	
		BSA	Lysozyme
K15-DW	149.0 ± 3.4	99.4 ± 0.2	59.8 ± 3.2
K15-WW	86.6 ± 1.7	99.5 ± 0.4	71.0 ± 4.5
K25-DW	44.2 ± 0.1	99.2 ± 0.1	57.9 ± 3.7
K25-WW	35.7 ± 3.3	99.4 ± 0.2	89.4 ± 4.1
K30-DW	30.6 ± 1.8	99.3 ± 0.3	82.9 ± 1.6
K30-WW	26.6 ± 0.8	99.3 ± 0.3	94.5 ± 1.7
K90-DW	6.5 ± 0.1	98.1 ± 1.1	86.4 ± 2.2
K90-WW	2.5 ± 0.2	98.4 ± 0.2	47.1 ± 9.0

decreased and the lysozyme rejection increased as the molecular weight of PVP increased. This is supported by the membrane morphologies shown in Figures 5–7 and other researchers' experimental results.^{18,25,30,34} According to the SEM images in Figure 5, the PES-C membranes prepared with low-molecular-weight PVPs as additives had large, fingerlike cavities and thin skin layers on both the external and internal surfaces, and this was favorable for water permeation. The results are similar to those for PAN membranes reported by Kang and Lee.²⁵ During precipitation, PVP is difficult to wash out completely from the membrane matrix. In particular, high-molecular-weight PVP is easily entrapped by the PES-C matrix.^{18,30} The PVP remaining in the polymer matrix blocks pores and impedes the permeation of water through the membrane. In addition, the investigations of Yang and Chung¹⁸ and Kang and Lee²⁵ revealed that the mean effective pore size of PES and PSf membranes decreases as the molecular weight of PVP increases. This decrease also can explain the decrease in the PWP flux and the increase in lysozyme rejection with the PVP molecular weight increasing. The results shown in Table II reveal that the BSA rejection values for the prepared PES-C membranes were all greater than 98%, and the lysozyme rejection values ranged from 47.1% to 94.5%. This illustrates that typical PES-C hollow-fiber UF membranes were fabricated in this case. Generally, permeation and separation performances are determined by the membrane structure and material properties. In this research, increasing the PVP molecular weight led to increased thickness and a reduction of fingerlike structures, as verified by the SEM images in Figures 5–7. This is similar to the effects on the evolution of the morphology and permeation performances of poly(vinylidene fluoride) membranes.³⁵

Moreover, the dry/wet-spun membranes had higher PWP flux values and lower lysozyme rejection values than the wet/wet-spun membranes. This phenomenon was also observed in PES hollow-fiber

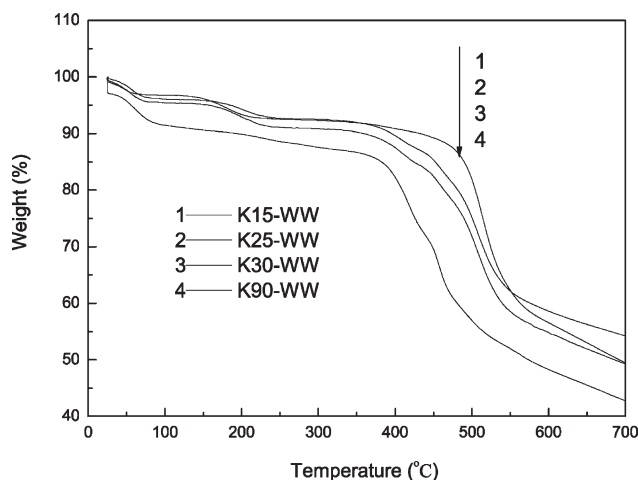


Figure 8 TGA curves of PES-C hollow-fiber membranes with different PVPs as additives.

membranes by Xu and Qusay¹³ and Qin et al.³⁶ Qin et al. claimed that with the air-gap distance increasing, the shear-induced orientation at external surfaces relaxed and loosened its tight structure; this yielded membranes with low rejection but high flux. All PES-C membranes in this case followed this rule, except for the lysozyme rejection of the K90-DW and K90-WW membranes. The much lower PWP flux of the membranes with PVP K90 as an additive should be the result of the spongelike structure, the much greater pore blocking of retained PVP, and the thicker skin layer.

Thermal properties

TGA curves of the wet/wet-spun PES-C hollow-fiber membranes are illustrated in Figure 8. There were three weight-loss stages for all the PES-C hollow-fiber membranes. This was similar to the thermal decomposition process of PES membranes.³⁷ The first weight loss below 100°C was attributed to the evaporation of water in the membranes. The second stage from 160 to 230°C was assigned to the loss of water or residual solvent in the membranes. The weight losses of the first stage (to 100°C) and the second stage (to 230°C) are listed in Table III. The weight loss of these two stages increased with

TABLE III
Weight Loss and T_d Values of the PES-C Hollow-Fiber Membranes

Membrane	Weight loss (%)		T_d (°C)
	100°C	230°C	
K15-WW	3.21	7.31	440.7
K25-WW	3.90	6.97	395.3
K30-WW	4.56	8.58	389.5
K90-WW	8.53	10.87	365.1

TABLE IV
Mechanical Properties of the PES-C Hollow-Fiber Membranes

Membrane	Break strain (MPa)	Elongation at break (%)
K15-WW	5.08 ± 0.35	9.19 ± 1.03
K25-WW	7.75 ± 0.05	12.60 ± 0.51
K30-WW	7.62 ± 0.09	18.57 ± 0.67
K90-WW	8.88 ± 0.16	29.30 ± 8.33

the molecular weight of PVP in the PES-C membranes. More PVP was retained in the membrane matrix when its molecular weight increased. Much more PVP was retained in the membrane matrix; more water was absorbed into the membranes, and greater weight loss occurred in the first two decomposition stages. The third stage from 360 to 450°C corresponded to the decomposition of the polymer. The values of the decomposition temperature (T_d), which is defined as the temperature at 3% weight loss (from 230°C), are also listed in Table III. The T_d values of the prepared PES-C membranes were all below the T_d value of the virgin polymer (460°C), and this was due to the existence of PVP in the membrane matrix. The deviation of T_d from the value of the virgin polymer was related to the molecular weight of PVP. T_d of the prepared PES-C membranes decreased when the molecular weight of PVP increased.

Mechanical properties

The mechanical properties of the wet/wet-spun PES-C hollow-fiber membranes were evaluated with the break strain and the elongation at break. The values are listed in Table IV. After consideration of the experimental error, the mechanical strain and elongation at break of the PES-C hollow-fiber membranes seemed to depend on the molecular weight of PVP. Both the break strain and the elongation at break increased when the molecular weight of PVP increased. The reason should be the suppression of the fingerlike cavities and the increasing thickness of the skin layers for the membranes prepared with high-molecular-weight PVP.³³

In comparison with the mechanical properties of PES hollow membranes,³⁸ the elongation at break of the PES-C hollow-fiber membranes was evidently low; on the contrary, the break strain was high. This resulted from differences in the molecular chains due to the introduction of rather bulky phenolphthalein groups for PES-C.

CONCLUSIONS

PES-C hollow-fiber membranes were fabricated by wet/wet and dry/wet (10-cm air gap) processes

with PVPs of different molecular weights as additives. The results revealed general instantaneous demixing phenomena, and the precipitation rate decreased as the PVP molecular weight increased. SEM images indicated that a double, fingerlike structure occurred in the PES-C hollow-fiber membranes containing PVP K15, PVP K25, or PVP K30 with instantaneous phase demixing. However, the PES-C membranes containing PVP K90 revealed a sponge-like structure because of the high viscosity of the dope solution and the low precipitation rate. The PWP flux decreased, but the lysozyme rejection increased for the PES-C membranes when the molecular weight of PVP in the membranes increased. The largest PWP flux of $149 \text{ L m}^{-2} \text{ h}^{-1} \text{ bar}^{-1}$ was acquired for the PES-C membrane with PVP K15 as an additive. The BSA rejection values for PES-C membranes were all greater than 98%, and the lysozyme rejection values ranged from 47.1% to 89.4%. T_d of the PES-C membranes decreased with the molecular weight of PVP increasing. The break strain and elongation at break were enhanced as the PVP molecular weight increased.

The authors thank Yang Hu and Yang Qian for their helpful suggestions.

References

- Mulder, M. *Basic Principles of Membrane Technology*; Kluwer Academic: Dordrecht, 1996.
- Takht Ravanchi, M.; Kaghazchi, T.; Kargari, A. *Desalination* 2009, 235, 199.
- Liu, K.; Zhang, H.; Chen, T. *Chin. Pat.* 85101721 (1986).
- Jia, L.; Xu, X.; Zhang, H.; Xu, J. *J Polym Sci Part B: Polym Phys* 1997, 35, 2133.
- Blanco, J. F.; Nguyen, Q. T.; Schaetzel, P. *J Membr Sci* 2001, 186, 267.
- Li, L.; Wang, Y. *J Membr Sci* 2005, 246, 167.
- Wang, M.; Wu, L.-G.; Mo, J.-X.; Gao, C.-J. *J Membr Sci* 2006, 274, 200.
- Wang, M.; Wu, L.-G.; Zheng, X.-C.; Mo, J.-X.; Gao, C.-J. *J Colloid Interface Sci* 2006, 300, 286.
- Lafrenière, L. Y.; Talbot, F. D. F.; Matsuura, T.; Sourirajan, S. *Ind Eng Chem Res* 1987, 26, 2385.
- Han, M. J.; Nam, S. T. *J Membr Sci* 2002, 202, 55.
- Torrestiana-Sanchez, B.; Ortiz-Basurto, R. I.; Brito-De La Fuente, E. *J Membr Sci* 1999, 152, 19.
- Wang, D.; Li, K.; Sourirajan, S.; Teo, W. K. *J Appl Polym Sci* 1993, 50, 1693.
- Xu, Z.-L.; Qusay, F. A. *J Membr Sci* 2004, 233, 101.
- Li, J.-F.; Xu, Z.-L.; Yang, H.; Feng, C.-P.; Shi, J.-H. *J Appl Polym Sci* 2008, 107, 4100.
- Chakrabarty, B.; Ghoshal, A. K.; Purkait, M. K. *J Membr Sci* 2008, 309, 209.
- Idris, A.; Mat Zain, N.; Noordin, M. Y. *Desalination* 2007, 207, 324.
- Susanto, H.; Ulbricht, M. *J Membr Sci* 2009, 327, 125.
- Yang, Q.; Chung, T.-S.; Weber, M. *J Membr Sci* 2009, 326, 322.
- Yang, Q.; Chung, T.-S.; Santoso, Y. E. *J Membr Sci* 2007, 290, 153.
- Yang, Q.; Chung, T.-S.; Chen, S. B.; Weber, M. *J Membr Sci* 2008, 313, 190.
- Ochoa, N. A.; Prádanos, P.; Palacio, L.; Pagliero, C.; Marchese, J.; Hernández, A. *J Membr Sci* 2001, 187, 227.
- Jung, B.; Yoon, J. K.; Kim, B.; Rhee, H.-W. *J Membr Sci* 2004, 243, 45.
- Guo, Q. *Eur Polym J* 1992, 28, 1049.
- Lang, W.-Z.; Xu, Z.-L.; Yang, H.; Tong, W. *J Membr Sci* 2007, 288, 123.
- Kang, J. S.; Lee, Y. M. *J Appl Polym Sci* 2002, 85, 57.
- Boussu, K.; Vandecasteele, C.; Van der Bruggen, B. *Polymer* 2006, 47, 3464.
- Boussu, K.; Van der Bruggen, B.; Vandecasteele, C. *Desalination* 2006, 200, 416.
- Li, J.-F.; Xu, Z.-L.; Yang, H. *Polym Adv Technol* 2008, 19, 251.
- Peng, N.; Chung, T.-S.; Wang, K. Y. *J Membr Sci* 2008, 318, 363.
- Chakrabarty, B.; Ghoshal, A. K.; Purkait, M. K. *J Membr Sci* 2008, 315, 36.
- Li, X.; Chen, C.; Li, J. *J Membr Sci* 2008, 314, 206.
- Khayet, M. *Chem Eng Sci* 2003, 58, 3091.
- Khayet, M.; García-Payo, M. C.; Qusay, F. A.; Zubaidy, M. A. *J Membr Sci* 2009, 330, 30.
- Xu, Z.-L.; Chung, T.-S.; Huang, Y. *J Appl Polym Sci* 1999, 74, 2220.
- Lang, W.-Z.; Guo, Y.-J.; Chu, L.-F. *Polym Adv Technol*, to appear.
- Qin, J. J.; Gu, J.; Chung, T.-S. *J Membr Sci* 2001, 182, 57.
- Li, Y. I.; Chung, T.-S. *Micro Meso Mater* 2008, 113, 315.
- Qin, J.; Chung, T.-S. *J Membr Sci* 1999, 157, 35.